STUDY ON BRAKING STABILITY OF MULTI-FRICTION DISC WET-TYPE BRAKE BASED ON THERMAL-FLUID-SOLID COUPLING

Mingchao Geng[1,2], Tiezheng Cui[1,2], Donghao Wu[1,2], Xukun Yin[3], Zhenxing Wang[1,2]*
[1]School of Mechanical Engineering, Hebei University of Architecture, Zhangjiakou, 075000, Hebei, China
[2]Hebei Technology Innovation Center for Intelligent Production Line of Prefabricated Building Components
[3]Hebei Guochuang Jingjinji Technology Development Co., Ltd, Shijiazhuang 050081, China
corresponding author: Zhenxing Wang
E-mail: wzx2124@hebiace.edu.cn

Abstract - Research on brake performance has been mainly focused on the improvement and optimization of the single performance of brakes. However, multi-factor and multi-dimensional safety optimization of brakes has become a crucial issue confronted in the current structural design of brakes. This study is aimed to reveal the dynamic interaction laws of multi-physical fields during the braking process of multi-friction discs, quantify the influence of key parameters on braking performance, and provide support for the optimal design of brakes. Finite element simulation models of thermal-fluid-solid coupling under three braking conditions (normal, intermediate and emergency) were established, and systematic analyses were carried out. Through these efforts, the key influencing effects of initial braking speed and oil temperature on braking performance were clarified. The revealed coupling laws can provide a theoretical basis for the selection of friction materials, structural optimization and improvement of heat dissipation systems of wet brakes, help enhance their thermal stability and service life under extreme working conditions, and thus possess significant engineering value.

Keywords: Wet Brake, Multi-field Coupling, Finite Element Analysis, Contact Mechanics of Friction Pairs, Braking Efficiency

1. Introduction

During the vehicle braking process, changes in brake performance are affected by multiple factors [1-3]. An analysis of vehicle brake performance is of great significance for ensuring vehicle safety. Studies on automotive braking performance have been conducted by several scholars. Wang et al. conducted research on PID control for braking control strategies [4] and found that the selection of an appropriate control strategy can significantly reduce the vehicle's braking distance. Jiang [5] et al. carried out a detailed study on the frictional performance of braking pavements and concluded that incorporating the road adhesion coefficient into braking conditions and comprehensively considering factors such as weather changes are of great value for the analysis of autonomous vehicle braking safety. In recent years, the adoption of the multi-field coupling finite element method to comprehensively evaluate automotive braking performance has become an important approach to improving vehicle braking performance. The classical theoretical studies on thermoelastic instability were pioneered by Dow [6]and Burton et al. [7], which lay the foundation for the analysis of hot spots and contact instability in brakes. On the basis of summarizing previous studies, Zhang et al. [8] analyzed the variation laws of temperature, stress and strain of automotive brakes during the thermal-fluid-solid coupling process, providing technical support for the structural optimization of brakes. Song et al. [9] analyzed faults of wet brakes and pointed out that changes in lubricating oil need to be concerned during the design process to maintain stable braking performance. Fan [10] designed the temperature rise and cooling structure of wet brakes and indicated that paying attention to the temperature rise and cooling issues of brakes is particularly crucial under frequent braking conditions. Kan et al. [11] discussed the degradation of braking efficiency caused by thermal fade and pointed out that reducing thermal fade is of great importance for automotive braking safety. To sum up, solving the problem of brake

dx.doi.org/10.17683/ijomam/issue24.31

thermal fade is of significant value for ensuring the constancy of braking effect.

To address the issue of brake thermal fade, Cui et al. [12] designed a new type of brake structure, which greatly improved the constancy of braking efficiency by optimizing the length of the lubricating oil cooling path. Zhang [13] conducted exploratory research on the optimization of the brake housing structure, improving the service life of the housing. Chen [14] carried out lightweight research on brake materials using the finite element method, which enhanced the service life of brakes. Tang et al. [15] optimized the interaction structure of brake pads, avoiding brake failure caused by thermal effects.

In summary, the improvement and enhancement of brake performance remain important contents for ensuring automotive braking safety at present. Currently, the multi-field coupling finite element method has important application value in the structural optimization and performance analysis of brakes [16-18]. Conducting research on the braking laws of brakes under different braking conditions is still an important approach to ensuring the constancy of braking efficiency.

2. Brake Coupling Control Methods

2.1 Theoretical Equations

During brake operation, compression and relative sliding occur between the friction pairs (friction pads and counter steel discs) under the action of braking pressure. The energy dissipated at the contact interface due to plastic deformation or micro-fracture of surface materials is primarily converted into thermal energy, thereby inducing a temperature rise at the friction interface. This process is defined as the frictional thermal effect. Based on tribological principles, the heat flux density generated per unit area and per unit time at the contact interface under sliding friction conditions can be expressed as:

$$q(x,y,t)=\mu v(x,y,t)p(x,y,t) \tag{1}$$

In the formula, q(x,y,t) denotes the heat flux density of the friction surface (W/m^2); μ represents the coefficient of friction between the friction pad and the steel disc; v(x,y,t) is the relative sliding velocity of the friction pair (m/s); and p(x,y,t) stands for the contact pressure of the friction pair (Pa).

Among the heat flux generated at the contact surface of the friction pair, most is absorbed by the friction pads and counter steel discs, and the other part is absorbed by media such as lubricating films and particles. If the proportion coefficient is set as δ, the following can be obtained:

$$q(x,y,t)\times\delta=\lambda_s\frac{\partial T_s}{\partial y}-\lambda_f\frac{\partial T_f}{\partial y} \tag{2}$$

In the formula, λ_s and λ_f denote the thermal conductivity of the counter steel disc and the friction pad, respectively. The temperature at the actual contact points on the friction interface is continuous, i.e.,

$$T_s(x,y,\mathrm{t})=T_f(x,y,\mathrm{t}) \tag{3}$$

where T_s and Tp represent the contact point temperatures of the counter steel disc and the friction pad, respectively (℃).

During brake operation, the generation of frictional heat flux is often accompanied by heat transfer phenomena, including heat conduction between friction pairs and other components, convective heat transfer with lubricating oil, and thermal radiation processes. Due to the relatively small influence of radiative heat dissipation under transient operating conditions, this factor is often neglected in the analysis. It can be seen that the temperature rise characteristics of the brake belong to a typical three-dimensional heat conduction problem, and the general expression of its heat conduction differential equation is:

$$\frac{\partial T}{\partial t}=\frac{\lambda}{\rho c}\left(\frac{\partial^2 T}{\partial x^2}+\frac{\partial^2 T}{\partial y^2}+\frac{\partial^2 T}{\partial z^2}\right)+\frac{\dot{\phi}}{\rho c} \tag{4}$$

In the formula, T denotes temperature (℃), t represents time (s); λ is thermal conductivity (W/(m·K)); ρ stands for density (kg/m^3); c denotes specific heat capacity (J/(kg·K)); and denotes the heat generation of the heat source per unit volume.

The physical meaning of this differential equation indicates that the change in internal energy within the control volume is equal to the vector sum of the spatial heat conduction input and the heat release from the internal heat source. To achieve the analytical solution of the transient temperature field T(x,y,z,t) of the brake using the heat conduction differential equation, the set of definite solution conditions must be clearly defined, including geometric configuration parameters, material property parameters, initial temperature field distribution, and the type of thermal boundary constraint. Thermal conduction boundary value problems are usually classified into three types of boundary conditions based on the constraint type.

The specification of boundary temperature values constitutes the first-type boundary conditions, and its relational expression under unsteady heat conduction scenarios is as follows:

$$T_w=f_1(t) \tag{5}$$

The specification of boundary heat flux density values is defined as the second-type boundary conditions, and the corresponding relational expression during the unsteady heat conduction process is as follows:

$$-\lambda\left(\frac{\partial T}{\partial n}\right)_w = f_2(t) \tag{6}$$

The specification of the surface heat transfer coefficient h between the object and the surrounding fluid at the boundary and the fluid temperature Tf is defined as the third-type boundary conditions. During unsteady heat conduction, both h and Tf can be expressed as functions of time t:

$$-\lambda\left(\frac{\partial T}{\partial n}\right)_w = h\left(T_w - T_f\right) \tag{7}$$

In the above formula, t denotes time (s), λ represents thermal conductivity, and Tw stands for the temperature on the boundary (℃).

2.2 Coupling Control Equations

The working process of the wet multi-disc brake studied in this paper involves three physical fields: thermal field, flow field, and solid structure field. As a typical mode of multi-field coupling, thermal-fluid-solid coupling integrates mechanical theories with disciplines such as heat transfer, thermodynamics, fluid mechanics, and solid mechanics. Its research scope includes thermal-solid coupled heat transfer problems, fluid-solid coupled deformation and motion problems, thermal-structural coupling problems, and thermal-fluid-solid three-field coupling problems. Its control equation system consists of fluid control equations, solid control equations, heat transfer control equations, and coupling control equations.

The basic control equations of fluid mechanics are composed of the continuity equation, momentum equation, and energy equation. According to the law of conservation of mass, the net mass flow rate of fluid entering the control volume per unit time is equal to the increasing rate of mass within the control volume, and the differential form of the continuity equation can be expressed as:

$$\frac{\partial \rho}{\partial t} + div(\rho \boldsymbol{V}) = 0 \tag{8}$$

Under steady flow conditions, fluid parameters do not change with time, i.e., $\frac{\partial \rho}{\partial t} = 0$. For incompressible fluids, the density ρ is constant, and the continuity equation is expressed as:

$$div(\boldsymbol{V}) = 0 \tag{9}$$

In the formula, ρ denotes fluid density (kg/m^3), t represents time (s), and V stands for velocity vector (m/s).

According to the law of conservation of momentum, the rate of change of momentum of a fluid element with time is equal to the sum of various external forces acting on the element, and the differential form of the momentum equation can be expressed as:

$$\rho \frac{D\boldsymbol{V}}{Dt} = \rho \boldsymbol{f} - div(p) + \mu \Delta \boldsymbol{V} \tag{10}$$

In the above formula, $\Delta = \frac{\partial^2}{\partial x^2} + \frac{\partial^2}{\partial y^2} + \frac{\partial^2}{\partial z^2}$, f is the mass force vector, p denotes pressure, and μ represents fluid viscosity.

According to the law of conservation of energy, the rate of energy increase within the fluid element is equal to the sum of the heat flow rate entering the fluid element and the work done by the mass force and surface force on the fluid element, and its mathematical expression is:

$$\frac{\partial(\rho T)}{\partial t} + div(\rho \boldsymbol{V} T) = div\left(\frac{k}{c} grad T\right) + \frac{S_T}{c} \tag{11}$$

In the formula, c denotes fluid specific heat capacity (J/(kg·K)), T represents temperature (℃), k is fluid thermal conductivity, and S_T stands for generalized source term. The control equation for solid vibration and displacement induced by fluid is as follows:

$$\boldsymbol{M}_s \frac{d^2 r}{dt^2} + C_s \frac{dr}{dt} + \boldsymbol{K}_s r + \tau_s = 0 \tag{12}$$

In the formula, M_s denotes the mass matrix, C_s represents the damping matrix, K_s stands for the stiffness matrix, r is the displacement of the solid, and τ_s denotes the stress acting on the solid. The basic heat transfer equation is as follows:

$$Q = kA\Delta t_{mn} \tag{13}$$

In the formula, k denotes the heat transfer coefficient (W/(m^2·K)), A represents the heat transfer area (m^2), and $\triangle t_m$ stands for the mean temperature difference of heat transfer (℃).

At the fluid-solid interface, the displacement, heat flux, temperature, stress, and other parameters of the fluid and the solid should be equal:

$$\begin{cases} n \cdot \tau_f = n \cdot \tau_s \\ r_f = r_s \\ q_f = q_s \\ T_f = T_s \end{cases} \tag{14}$$

In the formula, τ denotes stress (MPa), r represents displacement (mm), q stands for heat flux (J/s), T is temperature (℃), and the subscripts s and f denote solid and fluid, respectively.

2.3 Coupling Control Methods

Different coupling solution methods correspond to different engineering problems. For common thermal-fluid-solid coupling analysis problems of wet brakes, the braking conditions of the brake are often divided into three types for research, namely low-speed braking (Condition a), normal braking (Condition b), and emergency braking (Condition c). The braking characteristics and corresponding coupling control methods for each condition are shown in Table 1.

Table 1. Braking conditions and coupling methods

Conditions	Method	Basis
Condition a	Two-way Coupling Simulation	High vehicle speed, and the frictional heat simulation is sensitive.
Condition b and condition c	One-way Coupling Simulation	Low vehicle speed, both the fluid friction and braking stress brake are sensitive.

3. Finite Element Modeling of Brake Pads for Wet Brakes

3.1 Brake Friction Pad Modeling

The three-dimensional structural model of the wet brake is shown in Figure 1. Inside the brake housing, friction pads and counter steel discs are arranged alternately to form multiple sets of friction pairs. The enclosed lubricating oil in the housing flows from the inner diameter to the outer diameter through the grooves of the friction pads under the action of the centrifugal force of the rotating steel discs. Based on this, the complete groove structure of the friction pads must be retained during the simplification of the geometric model to accurately characterize the flow pattern of the lubricating oil and the convective heat transfer effect between the oil and the brake pads during the braking process. Considering that the size of the spiral groove structure of the friction pads is small, the number of model meshes is large, resulting in long calculation time and certain consumption of computing resources. A part of the brake friction pads is selected as the research object, and the area marked by the red wireframe is the modeling area of this section. Based on the assumption of symmetry on both sides of the friction pad and the steel disc, the mid-plane of the two is selected as the symmetric plane for heat flux analysis (heat flux is 0), the spline structure is retained, and the fillets are removed. Finally, the mesh geometric model of the friction pair and lubricating oil established in the Workbench software is shown in Figure 2.

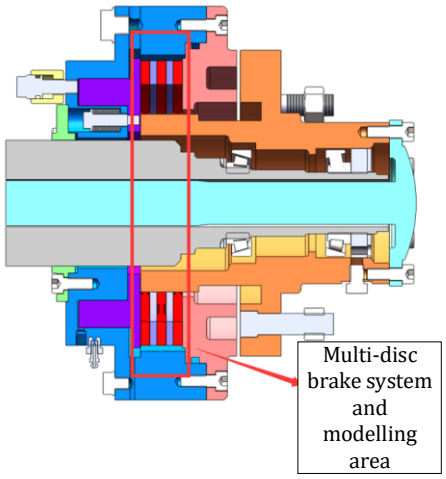

Figure 1: Friction Disc Model

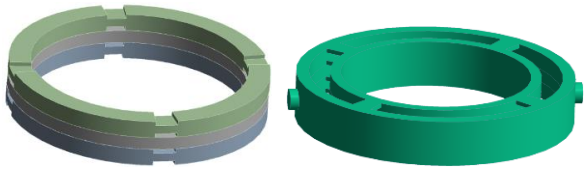

(a) Geometric Model of the Friction Pair(b) Geometric Model of the Lubricating Oil Channel

Figure 2: Geometric Models of the Friction Pair and Lubricating Oil

3.2 Mesh Generation and Boundary Definition

The thermo-mechanical coupling analysis of brake friction pads shows highly nonlinear characteristics. Convergence can only be achieved through repeated iteration, which makes the problem of computational efficiency rather prominent. To meet the high-precision requirements for dynamic contact pair elements, mesh refinement is performed in the vicinity of the axial contact area between the brake disc and friction pads, while the mesh is appropriately coarsened in regions away from the contact area. To improve the convergence rate, the mesh density of friction pads is set higher than that of the brake disc.

Given that under the same dimension, hexahedral elements have fewer element counts, faster solution speed and higher accuracy compared with tetrahedral elements, hexahedral elements are adopted for the solid components of wet multi-disc brakes, and quadrilateral elements are selected for rigid surfaces. Considering the requirements of thermo-mechanical coupling analysis, the tetrahedral element type is designated as C3D4 and the hexahedral element type is designated as C3D8RT. Eventually, a total of 5,637,861 elements and 1,075,794 nodes are generated, and the results of mesh generation are illustrated in Figure 3.

(a) Mesh of the Friction Pair (b) Mesh of the Lubricating Oil

Figure 3: Meshes of the Friction Pair and Lubricating Oil

After the completion of mesh generation, the coupled boundary conditions of the friction pads were defined, as shown in Figure 4. Both the steel plate-oil contact surface and the friction pad-oil contact surface were designated as two-way fluid-structure interaction interfaces, as indicated by the annotated areas in the figure. During the calculation process, the energy conservation equation was activated, and the pressure-velocity coupling algorithm was adopted to solve the Navier-Stokes equations. The convergence residual threshold was set to 1×10^{-5}.

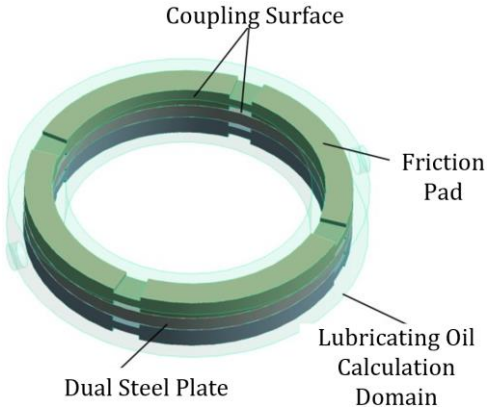

Figure 4: Boundary Condition Setup for the Thermal-fluid Coupling Model

In the Transient Structural software, material properties were assigned to the friction pads and mating steel plates respectively, and the constraints and loads of the brake pads were set in accordance with the braking characteristic curve.

Specifically, the braking pressure load was applied to the contact surface of the mating steel plates; displacement constraints were imposed on the inner circular surface; frictional contact conditions were defined on the contact surface with the friction pads; and axial support was provided on the other end surface. Meanwhile, the contact surfaces between the lubricating oil, friction pads and mating steel plates were designated as fluid-structure interaction interfaces, as shown in Figure 5.

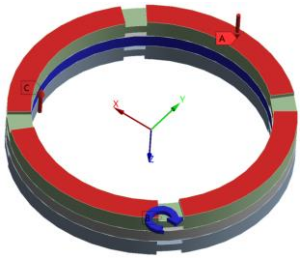

Figure 5: Loads and Constraints of the Friction Pair

3.3 Material Definition

The material property parameters of the friction pair of the wet multi-disc brake investigated are presented in Table 2. The properties of the relevant materials are taken from References [10], [19] and [20]. The brake housing is filled with ISOVG46 lubricating oil, and its material property parameters at 50 °C are listed in Table 3.

Table 2. Material Property Parameters of the Friction Pair

Material	45 Steel [10]	40Cr Steel [19]	Aramid Fiber Reinforced Phenolic Resin [20]
Elastic Modulus (GPa)	206	211	5
Poisson's ratio	0.3	0.3	0.27
Density (kg/m³)	7850	7820	6700
Thermal Conductivity λ(W/(m·K))	60.5	60.5	0.45
Specific Heat Capacity (J/ (kg· K))	434	477	460
Coefficient of Thermal Expansion (10^{-5}/K)	1.2	1.2	1.71

Table 3. Material Property Parameters of Lubricating Oil

Temperature (℃)	Density (kg/m³)	Specific Heat Capacity (J/(kg·K))	Thermal Conductivity (W/(m·K))	Dynamic Viscosity (kg/(m·s))
50	870.6	0.48	0.11	0.025009

The heat flux distribution coefficient δ at the braking friction pair interface is calculated and determined based on the thermal conductivity λ. By using the formula:

$$\sigma = \lambda_s / (\lambda_s + \lambda_f) \tag{15}$$

Substituting the material parameters yields δ = 0.993, indicating that 99.3% of the frictional heat flows into the counter steel disc and 0.7% into the friction pad.

In ANSYS Workbench, this coefficient is defined via the heat flow allocation parameter of the contact pair to ensure the accuracy of the temperature field calculation in the thermal-fluid-solid coupling simulation.

4. Analysis of Braking Results of Friction Pads Based on Thermal-Fluid-Solid Coupling

4.1 Thermal – Fluid - Solid Coupling Characteristics of Working Condition a

For Working Condition a (with an initial rotational speed of 2 rad/s and a braking duration of 0.5 s), the braking pressure and temperature distributions of the discs and pads are shown in Figures 6 and 7, respectively.

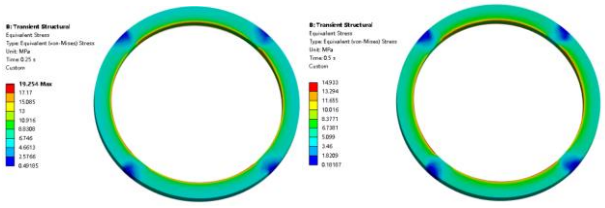

t=0.25s t=0.5s

Figure 6: Nephogram of Pressure Distribution of Discs and Pads at Different Time Instants

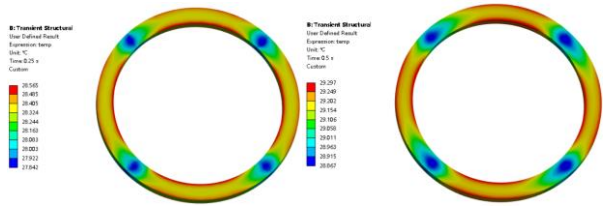

t=0.25s t=0.5s

Figure 7: Contour Plot of Temperature Distribution of Discs and Pads at Different Time Instants

It can be concluded from the above figures that the contact pressure between friction pads and mating steel plates was found to exhibit a uniform distribution characteristic at the initial stage of braking (0.25 s), with the maximum pressure value of 2.8 MPa concentrated in the central area of the contact surface. As the braking process proceeded to 0.5 s, the pressure distribution was gradually diffused toward the outer edge of the friction pads, and the peak pressure was reduced to 2.2 MPa. In terms of the temperature field, the central area of the contact surface reached a local peak temperature of 85 °C at 0.25 s. At 0.5 s, the temperature was decreased to 72 °C due to the convective heat dissipation effect of the lubricating oil. The overall temperature rise gradient was gentle, and no significant thermal stress concentration phenomenon was observed.

4.2 Thermal – Fluid - Solid Coupling Characteristics of Working Condition b

For Working Condition b (with an initial rotational speed of 6 rad/s and a braking duration of 0.5 s), the braking pressure and temperature distributions of the discs and pads are shown in Figures 8 and 9, respectively.

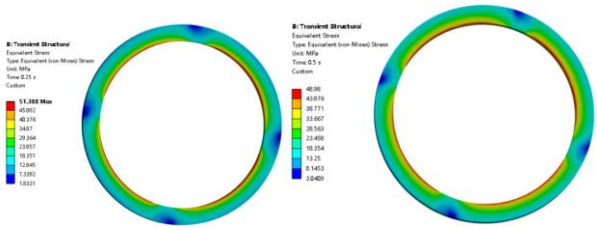

t=0.25s t=0.5s

Figure 8: Contour Plot of Pressure Distribution of Discs and Pads at Different Time Instants

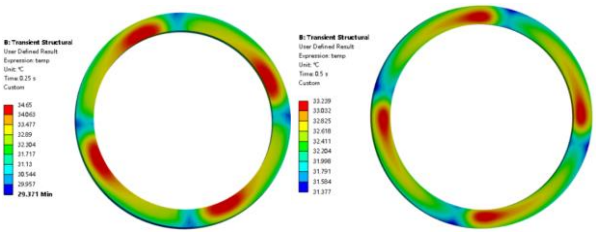

t=0.25s t=0.5s

Figure 9: Contour Plot of Temperature Distribution of Discs and Pads at Different Time Instants

It can be concluded from the above figures that the increase in the initial braking rotational speed leads to a higher sliding speed of the friction pair. The contact pressure reached a peak value of 4.5 MPa at 0.25 s, with a wider distribution range than that under conventional working conditions. At 0.5 s, the pressure distribution exhibited a tendency of edge concentration, with the peak pressure being 3.8 MPa. The evolution of the temperature field indicated that the temperature of the central area of the contact surface rose rapidly to 165 °C at 0.25 s, and then decreased to 138 °C at 0.5 s due to the circulating heat dissipation of the lubricating oil. However, the circumferential temperature gradient increased, which suggested the intensification of local thermoelastic deformation.

4.3 Thermal – Fluid - Solid Coupling Characteristics of Working Condition c

For Working Condition c (with an initial rotational speed of 12 rad/s and a braking duration of 0.5 s), the braking pressure and temperature distributions of the discs and pads are shown in Figures 10 and 11, respectively.

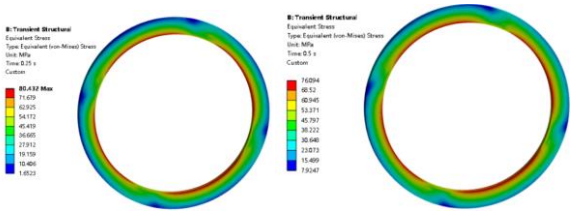

t=0.25s t=0.5s

Figure 10: Contour Plot of Pressure Distribution of Discs and Pads at Different Time Instants

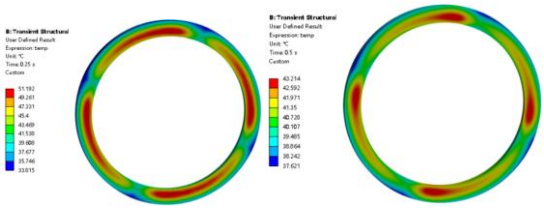

t=0.25s t=0.5s

Figure 11: Contour Plot of Temperature Distribution of Discs and Pads at Different Time Instants

It can be concluded from the above figures that the high sliding speed induced a surge in frictional heat flux. The contact pressure reached a peak value as high as 7.2 MPa at 0.25 s, and exhibited an asymmetric distribution characteristic, with obvious pressure concentration in the outer edge area of the contact surface. At 0.5 s, the peak pressure was still maintained at 6.5 MPa. The evolution of the temperature field was more intense: the temperature at the center of the contact surface soared to 320 °C at 0.25 s; due to the lag in heat dissipation of the lubricating oil, the temperature only decreased to 295 °C at 0.5 s. Both the circumferential and radial temperature gradients exceeded 200 °C/mm, which indicated that the risk of thermoelastic instability increased significantly under this working condition.

5. Effect of Braking Process on Lubricating Oil Temperature

Variations in the performance indicators of lubricating oil are regarded as important indices for evaluating changes in braking performance. The performance variations of the brake lubricating oil within the temperature range of 25 °C–45 °C are presented in the following table.

Table 4. Performance Characterization of Lubricating Oil Under Different Braking Temperatures

Temperature (°C)	Dynamic Viscosity ($\times 10^{-6}$ kg/(m·s))	Reynolds Number	Maximum Oil Temperature (°C)	Braking Contact Uniformity Coefficient
25	25009	1200	85	0.92
35	18000	1800	92	0.85
45	9500	2500	105	0.78

It is found from the analysis of the lubricating oil temperature and its performance variations that as the temperature of the brake lubricating oil increases, the braking performance decreases sharply, and the flow behavior of the lubricating oil gradually transforms from laminar flow to turbulent flow. The increased energy consumption of the brake fluid leads to a rise in its temperature, which in turn causes an increase in the braking temperature, thus forming a vicious cycle.

Meanwhile, from the perspective of the contact coefficient of the brake discs and pads, as the temperature rises and high temperatures are generated, the structure of the brake discs and pads may undergo changes. In the meantime, the elevated temperature of the lubricating oil may also result in the degradation of braking performance.

6. Conclusions

A numerical analysis framework for wet multi-disc brakes involving thermal-fluid-solid three-field coupling was established, and a coupling control strategy adapted to three braking conditions was proposed. A refined finite element model incorporating the groove structure of friction pads was constructed via Workbench software. The hybrid hexahedral/tetrahedral meshing (with mesh refinement in contact areas), two-way fluid-structure interaction boundary setup, and pressure-velocity coupling algorithm were adopted for solution. This work provides reliable methodological support for the multi-field coupling stability analysis of such brakes. The relevant results are consistent with those reported in Reference [21]. Compared with Reference [21], which only discusses thermal-structural coupling simulation, this paper further improves the thermal-fluid-solid coupling simulation method for brakes.

A systematic study on the thermal-fluid-solid coupling characteristics of wet multi-disc brakes was conducted, with a focus on analyzing the contact pressure distribution and temperature field evolution law of friction pairs under different braking conditions. The correlation mechanism between lubricating oil physical parameters (dynamic viscosity, thermal conductivity, etc.) and braking performance was clarified. Meanwhile, quantitative analysis of key contents such as the definition of friction pair material properties, load and constraint setup, and coupling boundary condition optimization was completed, which comprehensively covers the core technical links of the coupled operation of brakes.

The vicious coupling cycle law between oil temperature and braking performance during the braking process was revealed. A rise in oil temperature (from 25 °C to 45 °C) results in a 62% reduction in the dynamic viscosity of lubricating oil and an increase in the Reynolds number to the

critical value of turbulence, which further causes the braking contact uniformity coefficient to drop to 0.78 and the braking efficiency to attenuate significantly. Under different braking conditions, the higher the initial rotational speed, the larger the peak contact pressure, peak temperature of the contact surface, and thermal stress gradient of the friction pair. The risk of thermoelastic instability increases significantly under emergency braking conditions, which provides key data support for the structural optimization and condition adaptation of brakes.

Acknowledgement

The authors would like to acknowledge the support received from the following projects: Automobile Experiment (a specialized and innovation-integrated course) of the Innovation and Entrepreneurship Course Program of Hebei Province, Project **No. 2025cxkc118**; S&T Program of Hebei **NO. 25360801D**; and Graduate Innovation Fund Project of Hebei University of Architecture **NO. XP2025034.**

References

[1] Li, F., Deng, Y.T., Liu, Y.X., Zhou, S.Q. (2024) Safety Braking Strategies for Autonomous Vehicles Considering Road Friction Performance. Journal of Tongji University (Natural Science) 52(4), 489-500.

[2] Ren, Z.Y., Shi, Q., Yan, K. (2025) Analysis of Single Pedal Regenerative Braking Efficiency of Coal Mine Electric Vehicles. China Mechanical Engineering2), 209-219.

[3] Liuqian. (2024) The Influence of Automotive Brake Pad Materials on the Safety of Braking Systems. Automotive Test Report16), 59-61.

[4] Wang, S.H. (2025) Intelligent Adaptive PID Control Strategy for Torque During Emergency Braking Process of Electric Vehicles. Journal of Taiyuan Urban Vocational College11), 25-28.

[5] Huang, X.M., Jiang, Y.M., Zheng, B.S., Zhao, R.M. (2020) Theory and methodology on safety braking of autonomous vehicles based on the friction characteristic of road surface. Chinese Science Bulletin 65(30), 3328-3340.

[6] Dow, R. A., & Burton, R. A. (1972). Thermoelastic instability of sliding contact in the absence of wear. Wear, 19(3), 315–328.

[7] Burton, R. A., Nerlikar, V., & Kilaparti, S. R. (1973). Thermoelastic instability in sliding half-planes. Journal of Lubrication Technology, 95(4), 456–464.

[8] Zhang, C.W., Zhao, D.W., Liu, J.P. (2025) Analysis of Thermal Fluid Structure Coupling Temperature Field and Stress Field of Wet Multi Disc Brake. Machinery Design & Manufacture, (3), 152-158.

[9] Song, R.B. (2024) Fault Analysis for Hydraulic System of Wet Clutch Brake of A Hot Die Forging Press. China Heavy Equipment3), 17-20.

[10] Fan, J.P. (2023) Temperature rise analysis of braking condition of wet brake for mine-used flame-proof trackless rubber-tyred vehicle. Mining & Processing Equipment 51(8), 22-25.

[11] Kan, K.Y., Xiong, X., Shi, X.L., Sun, T.T., Zheng, Z. (2025) Research on Performance Optimization and Decay of Automobile Disc Brakes. Auto Time5), 157-159.

[12] Cui, Y.L., Shi, K., Wang, Y.H. (2024) Simulation and analysis of a new slow heat dissipation method for wet brakes. Agricultural Equipment & Vehicle Engineering 62(9), 33-38.

[13] Zhang, B. (2025) Optimization of the Brake Housing Structure of Mine Hoist Machinery. Mechanical Management and Development 40(9), 179-181, 184.

[14] Chen, X.S., Wang, Y.K., Zhang, T.S., Wang, Z.X., Zhang, J.K., Shi, F.F. (2025) Lightweight design and research of disc brake. Heavy Machinery, 84-89.

[15] Tang, J.R., Shang, H.L. (2024) Structural design optimization of ventilated brake disc based on extreme operating conditions. Journal of Technology 24(4), 426-431.

[16] Luo, H.J., Yan, B., Zhang, S. (2025) Finite Element Analysis of Thermal-Stress Coupling Relationship in Elevator Brake During Braking Process. China Elevator 36(2), 24-28, 32.

[17] Yan, Y.H., Wu, J.P., Cheng, R., Liu, X.P., Feng, C. (2025) Research and Analysis of Stress Field in Disc Brakes Based on Finite Element Method. Electric Engineering, (10), 22-24.

[18] Xiao, H. (2022) Finite Element Modal Simulation and Experimental Analysis of Disc Brake. Journal of Jiujiang University (natural sciences) 37(1), 22-24, 98.

[19] Chinese Mechanical Engineering Society. (2019). Mechanical Engineering Materials Handbook (Non-metallic Materials) [M]. Beijing: China Machine Press.

[20] Li Y, Li Y, Yang M, et al. (2015). ANALYZING THE THERMAL MECHANICAL COUPLING OF 40Cr COLD ROLL-BEATING FORMING PROCESS BASED ON THE JOHNSON–COOK DYNAMIC CONSTITUTIVE EQUATION. International Journal of Heat and Technology, 33(3):51-58.

[21] Wang, Z., & Zhang, J. (2021). In 6th International Conference on Design Engineering and Science (ICDES 2021). Journal of Physics: Conference Series, 1875. IOP Publishing Ltd.